

## N $\Delta$ -NN interaction in the pionic disintegration of the deuteron

H. Tanabe\*

*Institute for Nuclear Study, University of Tokyo, Tanashi, Tokyo 188, Japan*

K. Ohta

*Institute of Physics, University of Tokyo, Komaba, Tokyo 153, Japan*

(Received 27 July 1987)

The cross sections for the pionic disintegration of the deuteron in the  $\Delta$ -resonance region are calculated based on a unitary three-body model. The N $\Delta$ -NN transition potential is constructed from the  $\pi$ N  $P_{11}$  and  $P_{33}$  scattering amplitudes extrapolated to the off-shell region, and from the  $\pi$ NN three-body propagator. The idea of the two-potential model for the  $P_{11}$  wave is extended to the  $P_{33}$  wave. The parameters of the model are deduced from the fits to the  $\pi$ N scattering phase shifts. It is found that the off-shell  $P_{11}$  and  $P_{33}$  scattering amplitudes behave quite similarly to the monopole form factor with a cutoff momentum  $\Lambda = 600$  MeV/ $c$  as obtained earlier in the perturbation model by Gibbs, Gibson, and Stephenson. It is also found that the backward-propagating-pion component of the  $\pi$ NN propagator, which is often ignored in three-body calculations, is crucial to reproduce the magnitude of the total cross section. The three-body calculation is compared to the perturbation calculations. The second-order perturbation gives the results which closely approximate the full-order three-body calculation.

### I. INTRODUCTION

The pionic disintegration of the deuteron has drawn a great deal of interest as the basic process of pion annihilation in the nucleus. Experimental results for the total cross sections<sup>1</sup> show a pronounced broad peak in the vicinity of the energy of the  $\Delta$  resonance. This clearly indicates that the absorption of pions at intermediate energies is governed by the two step process,  $\pi d \rightarrow N\Delta \rightarrow NN$ .

Due to the very weak deuteron binding, the first step,  $\pi d \rightarrow N\Delta$ , is dominated by the quasifree  $\pi N \rightarrow \Delta$  vertex interaction. Since the magnitude of the  $\pi N \rightarrow \Delta$  vertex interaction in free space is directly related to the on-shell  $\pi N P_{33}$  scattering amplitude, there is little theoretical ambiguity in the calculation of the  $\pi d \rightarrow N\Delta$  amplitude. Differences in theoretical approaches arise from the different description of the N $\Delta \rightarrow NN$  transition amplitude; we may classify them into (i) perturbation models,<sup>2-11</sup> (ii) coupled channels models,<sup>12-15</sup> and (iii) unitary three-body models.<sup>16-21</sup>

In the perturbation models, the N $\Delta \rightarrow NN$  transition occurs through the exchange of a pion (and a  $\rho$  meson). The final state interaction is treated approximately using low-energy effective nucleon-nucleon interactions extrapolated up to the  $\Delta$  resonance region. Goplen, Gibbs, and Lomon<sup>2</sup> investigated the  $\pi d \rightarrow NN$  reaction based on the perturbation model with one-pion exchange and showed that the results are very sensitive to the choice of a cutoff factor at the  $\pi N\Delta$  vertex. To obtain agreement with the experimental total cross section they found a small cutoff momentum  $\Lambda = 300$  MeV/ $c$  [ $\Lambda$  refers to the monopole form factor  $(1 + q^2/\Lambda^2)^{-1}$  unless stated otherwise]. Shortly afterward Gibbs, Gibson, and Stephenson<sup>3</sup> showed that the  $\pi N\Delta$  cutoff momentum be-

comes considerably larger ( $\Lambda = 600$  MeV/ $c$ ) upon additional insertion of a cutoff at the  $\pi NN$  vertex.

The coupled channels calculation was first performed by Green and Niskanen.<sup>12</sup> The advantage of this approach is that it enables us to describe the final state NN interaction more realistically including all the iterations of the NN and N $\Delta$  states. In the  $\Delta$  resonance region NN scattering is known to be highly inelastic. The coupled channels models satisfactorily explain this phenomena based on the coupling of the N $\Delta$  states with the NN states.

Faddeev's three-body theory<sup>22</sup> was first applied to the  $\pi NN$  system by Afnan and Thomas.<sup>23</sup> This approach is often referred to as the unitary three-body model, since it satisfies the requirement of the two- and three-body unitarity. Theoretical inputs to the three-body equation are the two-body  $\pi N$  and NN interactions. Separable potentials are usually used to reduce the original Faddeev equation to the more tractable Faddeev-Lovelace<sup>24</sup> equation. The latter resembles the coupled channels equation. However, it should be emphasized that in the three-body models all the parameters of the two-body interactions (including the cutoff factors) are *fixed beforehand* by the two-body scattering data. This makes a sharp contrast with the perturbation or coupled channels models in which the cutoff factors are free parameters to adjust the magnitude of the N $\Delta \rightarrow NN$  transition amplitude.

Recent three-body calculations of the  $\pi d \rightarrow NN$  reaction have a tendency to underestimate the experimental cross sections. Lamot, Perrot, Fayard, and Mizutani<sup>21</sup> reported that a factor of about 4 is missing in the cross section compared with experiment. To circumvent this difficulty, they modified the off-shell  $\pi N P_{33}$  and  $P_{11}$  amplitudes in an *ad hoc* way. The connection with  $\pi N$

scattering is thus lost in their approach. At this point they overstepped the framework of the unitary three-body model. Afnan and McLeod<sup>20</sup> succeeded in getting a reasonable cross section at energies well above the  $\Delta$  resonance, but their prediction underestimates experiment near the  $\Delta$  resonance.

In this paper we attempt to resolve these discrepancies within the framework of the unitary three-body model and to get a consistent picture of the  $N\Delta$ -NN interaction. We have already performed three-body calculations for NN scattering<sup>25</sup> and have shown that the predictions for the inelastic cross sections are in good agreement with the data. As the two step process  $NN \rightarrow N\Delta \rightarrow \pi NN$  dominates the inelastic NN scattering, it seems to us that our model adequately reproduces the magnitude of the  $NN \rightarrow N\Delta$  transition amplitude. We expand our model space by introducing the  $\pi d$  channels in order to evaluate the  $\pi d \rightarrow NN$  cross section based on the unitary three-body model.

Concerning the  $N\Delta$ -NN interaction, there are two major different dynamical inputs between our model and other three-body models:

(i) We have introduced a nonresonant  $\pi N P_{33}$  interaction in addition to the  $\pi N \rightarrow$  bare  $\Delta \rightarrow \pi N$  resonant interaction. The off-shell behavior of the  $P_{33}$   $t$  matrix differs considerably from that of the standard  $\Delta$ -isobar model.

(ii) We have included a backward-propagating pion which is often neglected in the three-body calculation.

We estimate the effects of these inputs on the  $\pi d \rightarrow NN$  cross sections in comparison to different models. We also compare our three-body calculation with the perturbative calculation in order to estimate the importance of the multiple-scattering contributions.

Here we comment on the  $\rho$ -meson exchange contribution to the  $N\Delta$ -NN interaction. Brack, Riska, and Weise<sup>4</sup> calculated the  $\pi d \rightarrow NN$  cross section based on a perturbation model with pion and  $\rho$ -meson exchanges. They chose a strong  $\rho$ -nucleon tensor coupling constant which brought about very large cancellation between the pion- and  $\rho$ -meson-induced  $N\Delta$ -NN tensor interactions. They found that very hard form factors are required to reproduce the experimental total cross section ( $\Lambda = 1200$  MeV/ $c$  for  $\pi NN$  and  $\pi N\Delta$  vertices and  $\Lambda = 1800$  MeV/ $c$  for  $\rho NN$  and  $\rho N\Delta$  vertices).

Alternatively, Lee<sup>26</sup> used in his coupled channels calculation a weak  $\rho$ -nucleon tensor coupling constant and showed that the optimum cutoff for the  $\pi NN$ ,  $\pi N\Delta$ ,  $\rho NN$ , and  $\rho N\Delta$  vertices is  $\Lambda = 650$  MeV/ $c$ . If one chooses such a small cutoff momentum, the contribution of the  $\rho$ -meson exchange to the  $N\Delta$ -NN interaction becomes almost negligible, because it is a short range interaction in its nature. Moreover, Dmitriev, Sushkov, and Gaarde<sup>27</sup> analyzed the  $pp \rightarrow n\Delta^{++}$  reaction based on a perturbation model and showed that the angular distributions of the cross sections are highly sensitive to the choice of the cutoff factors. They concluded that the  $\pi NN$  and  $\pi N\Delta$  cutoff momentum should be  $\Lambda = 630$  MeV/ $c$  and the  $\rho$ -exchange contribution to the  $N\Delta$ -NN interaction is very small.

The standard unitary three-body model does not in-

clude the  $\rho$ -meson exchange, because we cannot fix the parameters of the  $\rho NN$  and  $\rho N\Delta$  vertex interactions by the two-body  $\pi N$  scattering data. Though there are some attempts<sup>18,19</sup> to supplement the  $\rho$ -exchange  $N\Delta$ -NN interaction to the three-body model, the present paper aims to study to what extent we can understand the  $\pi d \rightarrow NN$  reaction in the framework of the  $\pi$ ,  $N$ , and  $\Delta$  dynamics.

The organization of this article is as follows. Section II gives a brief summary of the unitary three-body equation as well as the parametrization of the two-body NN and  $\pi N$  interactions used in our calculation. We then describe the various choices for the dynamical inputs in Sec. III and give a series of results for the  $\pi^+ d \rightarrow pp$  reaction. Finally in Sec. IV, we present a summary of this work.

## II. UNITARY THREE-BODY MODEL

As mentioned in Sec. I, the Faddeev-Lovelace equation for the  $\pi NN$  system was first derived by Afnan and Thomas. It was then developed by Avishai and Mizutani,<sup>28</sup> Blankleider and Afnan,<sup>16</sup> and Rinat and Starkand<sup>18</sup> to include the nonpole part of the  $\pi N P_{11}$  interaction. We slightly rearrange this equation as

$$T^{\alpha\beta} = \sum_{\gamma} \left[ B^{\alpha\gamma} + \sum_d B^{\alpha d} G^d B^{d\gamma} \right] (\delta_{\gamma\beta} + G^{\gamma} T^{\gamma\beta}), \quad (1)$$

$$T^{Nd} = B^{Nd} + \sum_{\alpha} T^{N\alpha} G^{\alpha} B^{\alpha d}, \quad (2)$$

$$T^{dd} = \sum_{\alpha, \beta} B^{d\alpha} (\delta_{\alpha\beta} + G^{\alpha} T^{\alpha\beta}) G^{\beta} B^{\beta d}, \quad (3)$$

with  $\alpha, \beta, \gamma = N, \Delta$ . Here  $T$  are the three-body amplitudes,  $B$  the one particle exchange Born amplitudes (driving terms), and  $G$  the propagators of the two-body subsystem in the presence of a spectator. The index  $d$  refers to the  $\pi(NN)$  channel where the NN subsystem interacts in the  ${}^3S_1$ - ${}^3D_1$  or any other partial waves. In a similar manner,  $N$  corresponds to the  $(\pi N)N$  channel with  $\pi N$  interacting in the  $P_{11}$  partial wave, and  $\Delta$  represents all other  $(\pi N)N$  channels. Among the above three equations it suffices to solve only one integral equation, Eq. (1). Since  $d$  channels are decoupled from  $N$  and  $\Delta$  channels in this equation, we can reduce the number of effective coupled channels, thus making the numerical calculations much easier.

For the two-body NN interactions, we retain all the  $S$  and  $P$  partial waves, and  ${}^3D_1$  partial waves. We use the separable representation of the Paris potential<sup>29</sup> parametrized by Haidenbauer and Plessas.<sup>30</sup> Their non-relativistic amplitudes are translated into relativistic ones by the use of the standard method of relativization.<sup>31</sup> We have tried both of the rank 1 and rank 4 models for the  ${}^3S_1$ - ${}^3D_1$  interaction, but no significant difference has been detected. We choose the rank 1 model for simplicity.

For the  $\pi N$  interactions in the  $P_{11}$  and  $P_{33}$  partial waves, we take the two-potential models developed in our previous paper.<sup>25</sup> The interaction Hamiltonian  $V$  is the sum of the resonant interaction  $v_R$  and the background interaction  $v_B$ ,

$$V = v_R + v_B . \quad (4)$$

Assuming the existence of a bare particle, the resonant interaction is parametrized as

$$v_R = |v_1\rangle \lambda_1^{-1} \langle v_1| , \quad \lambda_1^{-1} = \frac{2m_0}{E^2 - m_0^2} , \quad (5)$$

where  $E$  and  $m_0$  are the  $\pi\text{N}$  total energy and the mass of the bare particle, respectively. The physical origin of the background interaction is most probably the crossed two-pion process, but we prefer to treat it as a purely phenomenological potential,

$$v_B = |v_2\rangle \lambda_2^{-1} \langle v_2| . \quad (6)$$

The transition amplitude is immediately obtained by solving the  $\pi\text{N}$  scattering equation,

$$t(E) = \sum_{i,j=1}^2 |v_i\rangle \tau_{ij}(E) \langle v_j| , \quad (7)$$

with

$$[\tau(E)^{-1}]_{ij} = \lambda_i \delta_{ij} - \sigma_{ij}(E) , \quad (8)$$

$$\sigma_{ij}(E) = \langle v_i | G_0(E) | v_j \rangle . \quad (9)$$

The parameters were fitted to reproduce the  $P_{11}$  and  $P_{33}$  phase shifts<sup>32</sup> up to  $T_\pi = 400$  MeV (in the  $P_{11}$  partial wave, the parameter search was done under the two constraints on the physical nucleon mass  $m_N$  and the physical  $\pi\text{NN}$  coupling constant  $f^2$ ). Phase shifts were not enough to fix all the parameters uniquely. We therefore constructed three parametrizations  $A$ ,  $B$ , and  $C$ , for each of the  $P_{11}$  and  $P_{33}$  interactions. The three models are characterized by the range of the resonant interaction  $v_1$ . Model  $A$  refers to the dipole form factor  $(1 + q^2/\Lambda^2)^{-2}$  with  $\Lambda = 1000$  MeV/ $c$  ( $\Lambda/\sqrt{2} \sim 700$  MeV/ $c$  if interpreted as a monopole form factor). The range is very close to the size of the proton.<sup>33</sup> Model  $B$  has the monopole form factor with  $\Lambda = 1200$  MeV/ $c$ . Such a short range form factor is found, for example, in the  $\pi + \rho$  model of Brack, Riska, and Weise.<sup>4</sup> Model  $C$  for the  $P_{33}$  channel corresponds to the conventional  $\Delta$ -isobar model<sup>34</sup> which lacks for the background interaction  $v_B$ . It predicted too small  $\text{NN} \rightarrow \pi\text{NN}$  cross sections<sup>25</sup> since the cutoff momentum at the  $\pi\text{N}\Delta$  vertex is very small ( $\Lambda/\sqrt{2} \sim 366$  MeV/ $c$ ;  $\Lambda$  for the dipole form factor). We do not use model  $C$  in the present calculation. The consequence of the soft  $\pi\text{N}\Delta$  form factor will be investigated in Sec. III C.

The  $\pi\text{N}$  interactions in the small partial waves,  $S_{11}$ ,

$S_{31}$ ,  $P_{13}$ , and  $P_{31}$ , are parametrized as rank 1 separable potentials. In momentum space  $|v\rangle$  is expressed as

$$\langle \mathbf{q} | v \rangle = v(q) \langle 1\mu_{\pi\frac{1}{2}}\mu | I\mu' \rangle \langle Lm_L \frac{1}{2}m | Jm' \rangle Y_{Lm_L}(\hat{\mathbf{q}}) , \quad (10)$$

where  $v(q)$  is the form factor.  $m_L$ ,  $m$ , and  $m'$  are the third components of the relative ( $L$ ), spin ( $S = \frac{1}{2}$ ), and total ( $J$ ) angular momentum, while  $\mu_\pi$ ,  $\mu$ , and  $\mu'$  are those of the pion, nucleon, and total isospin ( $I$ ), respectively.

The loop integral  $\sigma(E)$  is explicitly written as

$$\sigma(E) = \int_0^\infty dq \frac{m_N q^2 v^2(q)}{2(2\pi)^3 \omega_q E_q} G_0(q; E) , \quad (11)$$

where

$$E_q = (q^2 + m_N^2)^{1/2}$$

and

$$\omega_q = (q^2 + m_\pi^2)^{1/2} ,$$

and  $m_N$  and  $m_\pi$  are the physical nucleon and pion masses, respectively. For the  $\pi\text{N}$  propagator  $G_0$ , we choose the Blankenbecler-Sugar type,

$$G_0(q; E) = \frac{2(E_q + \omega_q)}{E^2 - (E_q + \omega_q)^2 + i\epsilon} . \quad (12)$$

The form factor  $v(q)$  is parametrized as follows:

$$v(q) = \left[ \frac{q}{m_\pi} \right]^L \sum_{n=1}^N f_n \left[ \frac{\Lambda_n^2}{\Lambda_n^2 + q^2} \right]^2 , \quad N = 1 \text{ or } 2 . \quad (13)$$

For the repulsive  $S_{31}$ ,  $P_{13}$ , and  $P_{31}$  waves we set  $\lambda = m_\pi$ , while for the attractive  $S_{11}$  wave we take  $\lambda$  to be energy dependent,  $\lambda = (E^2 - m_0^2)/2m_0$ , in order to reproduce the resonancelike feature at high energies. The above parameters are searched to fit the observed phase shifts for energies  $T_\pi < 400$  MeV. We present the results of the least square fitting in Table I.

Aaron, Teplitz, Amado, and Young<sup>35</sup> pointed out that the standard three-body model has a problem of lacking the pion propagation in the backward direction. The pion exchange propagator  $G_{\pi\text{NN}}$  appears in the driving term  $B^{\alpha\beta}$  as

$$\begin{aligned} \langle \mathbf{p}' | B^{\alpha\beta}(W) | \mathbf{p} \rangle \\ = C^{\alpha\beta} \langle v^\alpha | \mathbf{q} \rangle \langle \mathbf{p}' | G_{\pi\text{NN}}(W) | \mathbf{p} \rangle \langle \mathbf{q}' | v^\beta \rangle , \end{aligned} \quad (14)$$

TABLE I. Parameters for the small  $\pi\text{N}$  partial waves.

	$n$	$f_n$	$\Lambda_n$ (MeV/ $c$ )	$m_0$ (MeV)
$S_{11}$	1	7.9413	564.268	1474.97
$S_{31}$	1	10.5108	1513.18	
	2	-4.449 39	301.949	
$P_{13}$	1	1.815 45	649.076	
$P_{31}$	1	2.790 67	860.901	

where  $W$  is the total energy,  $\mathbf{p}$  and  $\mathbf{p}'$  are the initial and final momenta of the spectator nucleon, and  $\mathbf{q}$  and  $\mathbf{q}'$  are the  $\pi N$  relative momenta written in terms of  $\mathbf{p}$ ,  $\mathbf{p}'$ , and  $W$ .  $C^{\alpha\beta}$  is the constant factor which accounts for antisymmetrization.  $G_{\pi NN}$  is the sum of the forward and backward propagators,

$$\langle \mathbf{p}' | G_{\pi NN}(W) | \mathbf{p} \rangle = G_{\pi NN}^{(F)}(\mathbf{p}', \mathbf{p}; W) + G_{\pi NN}^{(B)}(\mathbf{p}', \mathbf{p}; W), \quad (15)$$

where

$$G_{\pi NN}^{(F)}(\mathbf{p}', \mathbf{p}; W) = \frac{E_p + E_{p'} + \omega_{p+p'}}{\omega_{p+p'} [W^2 - (E_p + E_{p'} + \omega_{p+p'})^2 + i\epsilon]}. \quad (16)$$

For  $G_{\pi NN}^{(B)}$  we take one half of the static pion propagator,

$$G_{\pi NN}^{(B)}(\mathbf{p}', \mathbf{p}; W) = -\frac{1}{2\omega_{p+p'}^2}. \quad (17)$$

This term ensures that  $G_{\pi NN}$  has the correct static limit and yet it does not violate the three body unitarity.

### III. RESULTS

With the above two-body NN and  $\pi N$   $t$  matrices as inputs, our three-body model reproduces the  $\pi d \rightarrow NN$  cross sections fairly well around the peak of the  $\Delta$  resonance. However, the calculated cross sections turn out to be too large at lower energies ( $T_\pi < 50$  MeV). In this region, the total cross sections are seriously deteriorated by the pion  $S$  wave rescattering process. As is seen in Table I, our cutoff factor for the  $S_{31}$  partial wave contains a very high momentum component ( $\Lambda_1 = 1513$  MeV/ $c$ ), which leads to the enhancement of the total cross sections. We will discuss this problem in Sec. III D. At the first stage of our calculations, we do not include the  $\pi N$   $S$  waves.

#### A. Three-body calculations

We have expanded the model of the previous paper by including the  $S$ ,  $P$ , and  ${}^3D_1$  NN interactions and the  $P_{13}$  and  $P_{31}$   $\pi N$  interactions. The essential ingredient of this extension is the inclusion of the  $\pi d$  channel. Mizutani *et al.*<sup>36</sup> and van Faassen and Tjon<sup>15</sup> have reported that the effect of the  $\pi d$  coupling is conspicuous in the NN scattering inelasticities near the pion production threshold. As is seen in Fig. 1, the model which includes only  $P_{33}$  and  $P_{11}$  partial waves (the original version) underestimates the  ${}^1D_2$  inelasticity at  $T_L < 700$  MeV. The extended model almost completely fills this discrepancy. On the contrary, the  $\pi d$  coupling does not increase the  ${}^3F_3$  inelasticity so much as the  ${}^1D_2$ . This reflects the  ${}^1D_2$  dominance of the  $\pi d \rightarrow NN$  reaction, which is established by the experimental partial wave analyses.<sup>38,39</sup>

The discrepancy of the  ${}^3F_3$  inelasticity around  $T_L = 800$  MeV is not remedied by the coupling to the  $\pi d$  channel. Many other model calculations<sup>26,36,40,41</sup> also failed to reproduce sufficient inelasticity in this wave. This is one of the important problems yet to be solved.

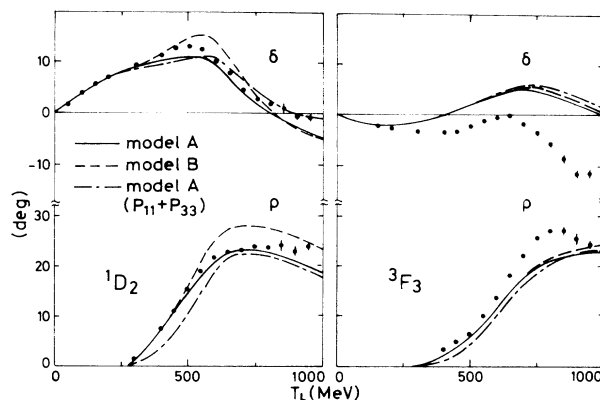


FIG. 1. Energy dependence of the NN scattering phase shifts for the  ${}^1D_2$  and  ${}^3F_3$  channels. The solid and dashed curves give the predictions of models  $A$  and  $B$ , respectively. The dash-dot curves represent the results of our previous calculations (model  $A$ ), which include only  $P_{33}$  and  $P_{11}$  partial waves. The data are from the analysis of Ref. 37.

We present in Fig. 2 the results for the  $\pi^+ d \rightarrow pp$  total cross sections. The shape and magnitude of the cross section in the resonance region are fairly well reproduced. It is not surprising that the predictions fall below the data at very low energies as we have neglected the  $\pi N$   $S$  wave interactions. Compared with model  $A$ , model  $B$  provides better results in the resonance region. However, this might be fortuitous, since model  $B$  overestimates the  ${}^1D_2$  inelasticity around the peak energy of the  $\pi^+ d \rightarrow pp$  reaction ( $T_L \sim 600$  MeV), while it underestimates the  ${}^3F_3$ .

The differential cross section  $d\sigma/d\Omega$  for the  $\pi^+ d \rightarrow pp$  reaction and the analyzing power  $A_{y0}$  for the  $\bar{p}p \rightarrow \pi^+ d$  reaction are shown in Figs. 3(a) and (b). The calculated differential cross sections agree reasonably well with experiment at energies below the  $\Delta$  resonance,

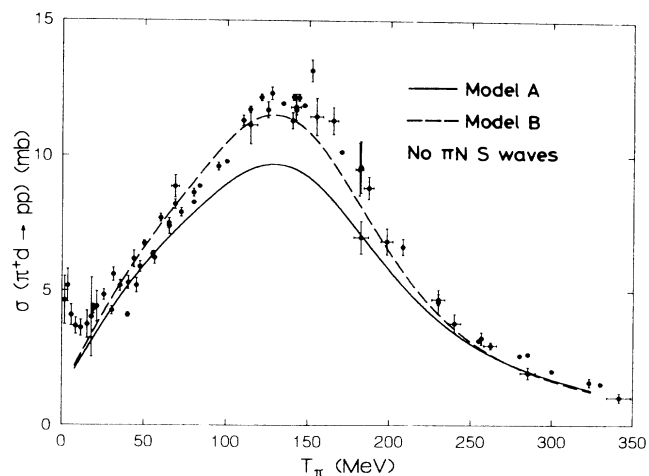


FIG. 2. Energy dependence of the total cross section for  $\pi^+ d \rightarrow pp$ . Models  $A$  and  $B$  do not include the  $S$  wave  $\pi N$  interactions. The data are from the compilation of Ref. 42.

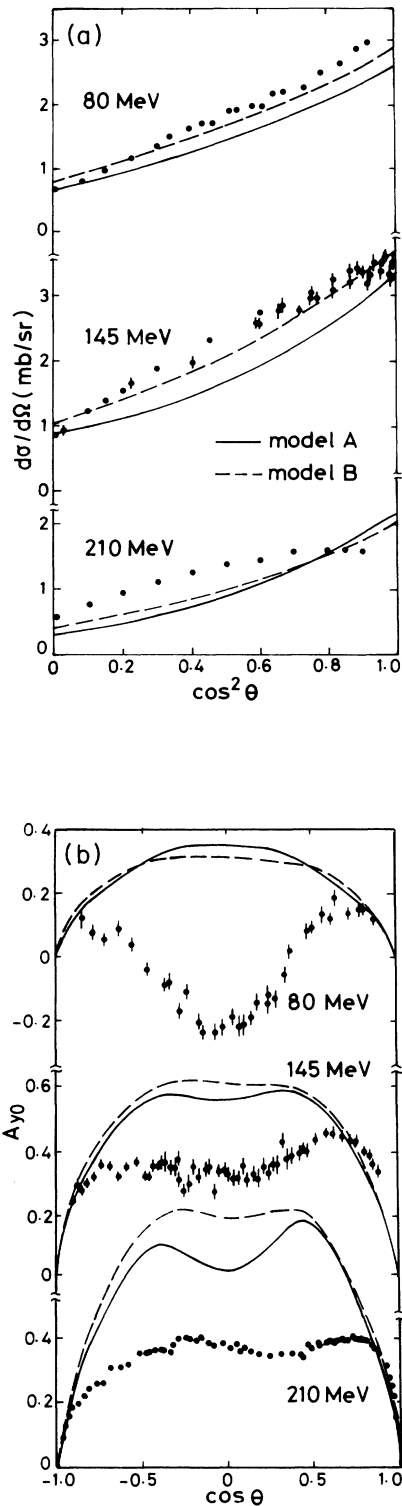


FIG. 3. (a) Angular distributions of the  $\pi^+d \rightarrow pp$  differential cross sections at  $T_\pi = 80, 145,$  and  $210$  MeV. The data are from Refs. 43–45. (b) Angular distributions of the analyzing power  $A_{y0}$  for the  $\bar{p}p \rightarrow \pi^+d$  reaction. The energies in the figure correspond to the pion kinetic energies for the inverse reaction  $\pi^+d \rightarrow pp$ . The data are from Refs. 46 and 47.

but become too forward peaked at higher energies. Afnan and McLeod<sup>20</sup> claim that the  $S$  and  $P$  wave NN interactions in the  $\pi(NN)$  channel considerably improve the shape of the angular distribution. Contrary to their results, we could not get the curvature of the differential cross sections correct, though we have included all the  $S$  and  $P$  wave NN interactions. As concerns  $A_{y0}$ , the calculated curves lie high above the experimental points. The features virtually coincide with the results obtained by Lamot *et al.*<sup>21</sup> The quantities related to the polarization are highly sensitive to fine details of theoretical models. There was an attempt to understand  $A_{y0}$  by the introduction of short range interaction.<sup>9</sup> Such a direction may be also relevant to our model.

### B. Perturbative calculations

In Fig. 4 the results for the first- and second-order perturbative calculations are displayed along with the three-body (full-order) calculation. In these calculations we have used model  $A$ . For the second-order process, we retain only the  $P_{33}$  rescattering term [diagram (b)].

The direct absorption process [diagram (a)] is strongly suppressed by kinematics, because the nucleons weakly bound in the deuteron cannot easily absorb the real pion. The  $P_{33}$  rescattering dominates the total cross section, but the interference with the direct absorption gives a non-negligible contribution. The interference term increases the total cross section and shifts the peak position to lower energy. The gross features of the cross section are reproduced by the second-order perturbation (direct absorption plus  $P_{33}$  rescattering). The higher-order contributions decrease the peak value by  $\sim 20\%$  and move the peak to further lower energy.

In these calculations we have used the off-shell  $P_{33}$  and  $P_{11}$  amplitudes determined by the  $\pi N$  scattering data. As mentioned in Sec. I, in the perturbation models the  $\pi N\Delta$  and  $\pi NN$  form factors are fixed by the

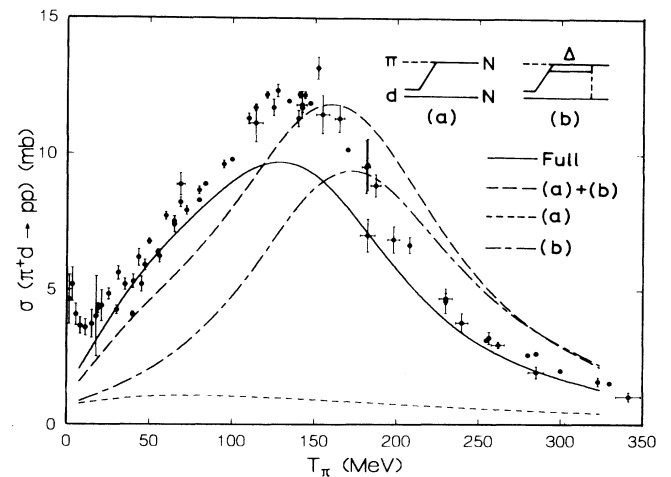


FIG. 4. Comparison of the perturbative and the full-order calculations for the  $\pi^+d \rightarrow pp$  total cross section. All four curves refer to model  $A$ . The data are the same as in Fig. 2.

$\pi^+d \rightarrow pp$  total cross sections. Gibbs, Gibson, and Stephenson<sup>3</sup> found that the monopole form factor with  $\Lambda = 600$  MeV/c is optimum to obtain the agreement with the data.

As we use the two-potential model for  $P_{33}$  and  $P_{11}$  scatterings, the off-shell behavior of the  $t$  matrices are determined by the complicated interplay between the resonant and background interactions. We therefore compare our model with the perturbation model in the form of the half-off-shell function

$$f(q, k) = \frac{R(q, k)}{R(k, k)} \left[ \frac{k}{q} \right]^L, \quad (18)$$

where  $R$  is the reaction matrix and  $k$  is the on-shell momentum. In the perturbation model, the half-off-shell function is reduced to the ratio of the off-shell and on-shell form factors,

$$f(q, k) = \frac{\Lambda^2 + k^2}{\Lambda^2 + q^2} \quad (19)$$

(perturbation model).

As is seen in Figs. 5(a) and (b), the half-off-shell functions show a striking resemblance among models *A* and *B* and the perturbation model of Gibbs, Gibson, and Stephenson. It is remarkable that the half-off-shell function derived from the analyses of the  $\pi N$  scattering data can be simulated by the form factor found in the perturbation model. From the figure we also see that the harder form factor ( $\Lambda = 1200$  MeV/c) in the perturbation model is incompatible with our model of  $\pi N$  scatterings.

### C. $N\Delta$ -NN interaction

We have seen that the second-order perturbation calculation gives the results which closely approximate the full-order three-body calculation. In this subsection all the calculations are done up to second order. The higher-order contributions are neglected in order to clarify the role of the  $N\Delta$ -NN interaction.

First we examine the effect of the backward-pion propagation [Eq. (17)]. As is seen in Fig. 6, excluding the backward propagator reduces the peak value of the total cross section about 60% (compare the solid curve with the long-dashed curve). Though many of the three-body calculations neglect the contribution of the backward-going pion, this term is indispensable in obtaining meaningful results for the  $\pi d \rightarrow NN$  cross section.

Next we study the effects of the off-shell  $P_{11}$  and  $P_{33}$   $t$  matrices. Figure 6 contains the perturbative calculations with the same inputs as Lamot *et al.*<sup>21</sup> (the dot-dashed curve), Afnan and McLeod<sup>20</sup> (the short-dashed curve), and Blankleider and Afnan<sup>16</sup> (the dotted curve). All of the above three models do not include the backward-propagating pion. We do not show here the results of the Weizmann Institute<sup>18</sup> or the Osaka University group,<sup>19</sup> because their models contain the  $\rho$ -meson exchange and it is beyond the scope of this article.

The corresponding  $P_{11}$  and  $P_{33}$  half-off-shell functions are shown in Figs. 7(a) and (b). As regards the  $P_{11}$ , the

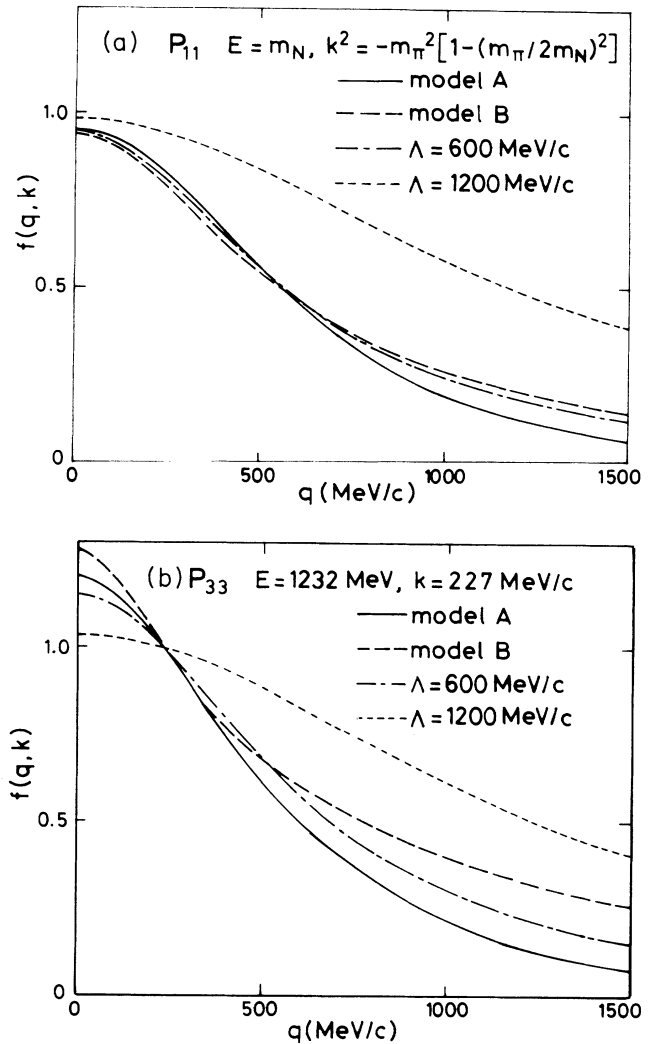


FIG. 5. Half-off-shell functions for the  $P_{11}$  and  $P_{33}$  partial waves.

curves of model *A*, Mizutani *B*,<sup>48</sup> and Afnan-McLeod *P6* lie close to each other, whereas the three models differ largely in the  $P_{33}$  partial wave. Lamot *et al.* resort to the conventional  $\Delta$ -isobar model which, as observed in Sec. II, yields a very soft  $\pi N\Delta$  form factor ( $\Lambda \sim 300$  MeV/c). The use of this form factor strongly suppresses the  $N\Delta \rightarrow NN$  transition and brings about the reduction of the  $\pi^+d \rightarrow pp$  cross section. The calculation underestimates experiment by a factor of about 4 and is consistent with the results of Lamot *et al.*

Afnan and McLeod utilize the  $P_{33}$  model of Thomas.<sup>49</sup> In his model a simple separable parametrization is used without assuming the existence of a bare  $\Delta$ . The form factor in this model has to be multiplied by a factor  $\sqrt{2\omega_q}$ , because the normalization factor of the pion  $\sqrt{2\omega_q}$  is effectively absorbed into the form factor. As is seen in Fig. 7(b), the form factor contains a component of very short range which is responsible for the enhancement of the  $\pi^+d \rightarrow pp$  total cross section. This effect partially compensates for the lack of the

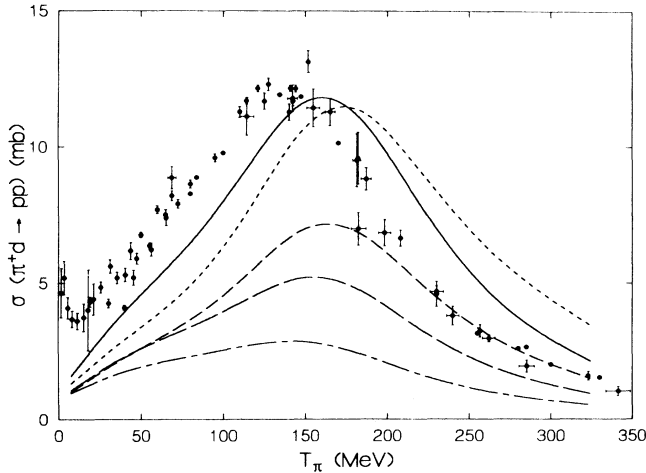


FIG. 6. Model dependence of the second-order perturbative calculation for the  $\pi^+d \rightarrow pp$  total cross section. Both the solid and long-dashed curves adopt model A, but the latter excludes the contribution of the backward-propagating pion. All the other three calculations do not include the effect of the backward-pion propagation. The dash-dot, short-dashed, and dotted curves refer to the models of Lamot *et al.* (Ref. 21), Afnan and McLeod (Ref. 20), and Blankleider and Afnan (Ref. 16), respectively.

backward-propagating pion. The three-body calculations of Afnan and McLeod were successful in reproducing the experimental cross section at  $T_\pi = 256$  MeV but failed at  $T_\pi = 140$  MeV. The features qualitatively agree with our second-order perturbative calculation. It may be difficult to seek the dynamical origin of such a complicated form factor, as the observed magnetic form factor of  $\Delta$  shows a smooth dependence on the momentum transfer.<sup>33</sup>

Blankleider and Afnan also use the  $P_{33}$  model of Thomas, but there is another factor in their input which enhances the  $\pi^+d \rightarrow pp$  cross section. We can see in Fig. 7(a) that the  $P_{11}$  half-off-shell function of Blankleider and Afnan is quite distinct from the other three. We suppose this is due to the fact that they did not fit the  $\pi NN$  coupling constant as well as the  $P_{11}$  phase shifts at high energies ( $T_\pi > 250$  MeV). For the same reason as stated before, we have multiplied their form factor by  $\sqrt{2\omega_q}$ . This factor emphasizes the slow damping of the form factor in the high momentum region which was already apparent in their original article (see Fig. 7 of Ref. 16). The three-body calculation of Blankleider and Afnan almost completely reproduces the experimental total cross section and roughly coincides with our perturbative calculation. It appears that if we append the effect of the backward propagating pion, we will overshoot experiment.

#### D. Influence of the $\pi N S$ waves

Figure 8 shows the results of the three-body calculations which assess the contributions of the  $\pi N S$  wave. The model with the  $S$  wave overestimates experiment at

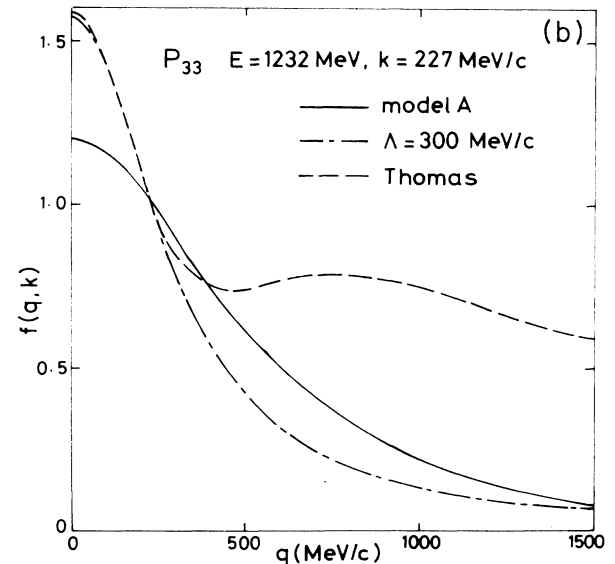
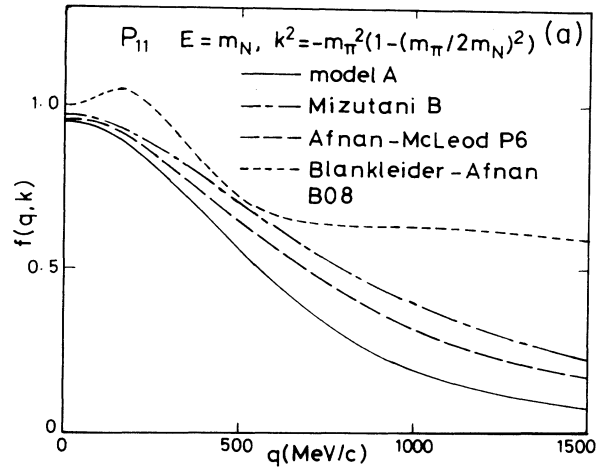


FIG. 7. Model dependence of the half-off-shell function for the  $P_{11}$  and  $P_{33}$  partial waves. The  $P_{11}$  half-off-shell function of Blankleider-Afnan B08 is normalized to one at  $q=0$  as we have multiplied their form factor by  $\sqrt{2\omega_q}$ .

low energies. We note that a similar observation was made by Vogelzang, Bakker, and Boersma.<sup>11</sup> The cause of the discrepancy is traced back to the anomalous behavior of the  $S_{31}$  form factor which we present in Fig. 9 compared with the results obtained by other groups.<sup>18,49,50</sup> We see that all the form factors have a large bump at  $q \sim 400$  MeV/c. It seems that this bump contributes to increasing the magnitude of the  $S_{31}$  wave rescattering amplitude.

We have tried to reduce this bump by exploiting a different parametrization for the  $S_{31}$  partial wave, but it has given no significant improvement. In our opinion, the problem resides in the separable approximation for the  $S$  wave interactions. As the  $S$  wave scatterings are strongly affected by the short range interaction, we

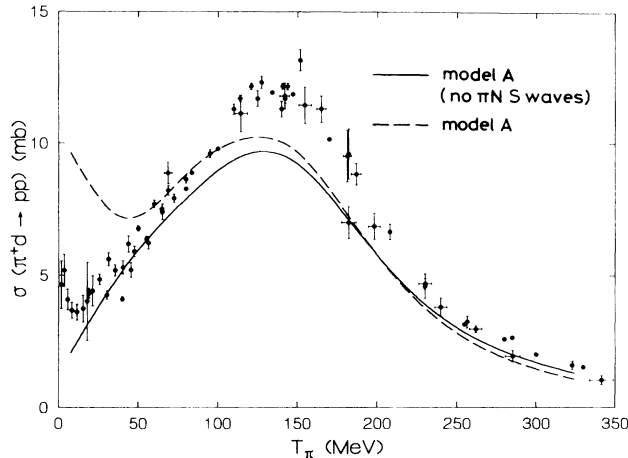


FIG. 8. Effect of the  $S$  wave  $\pi N$  interactions. The solid (dashed) curve excludes (includes) the contributions of the  $\pi N$   $S$  waves. The data are the same as in Fig. 2.

should employ more sophisticated parametrization for these waves.

#### IV. SUMMARY

We have investigated the  $N\Delta$ - $NN$  interaction through the calculation of the  $\pi d \rightarrow NN$  reaction. We have restricted the  $N\Delta$ - $NN$  interaction to the one-pion exchange sector. The strength of the pion exchange potential is controlled by the off-shell amplitudes of the  $\pi N$   $P_{33}$  and  $P_{11}$  partial waves and the propagator  $G_{\pi NN}$ .

The contribution of the backward pion propagator  $G_{\pi NN}^{(B)}$  is found to be very large. If we leave out this term, the cross section decreases about 60%. One of the reasons why the traditional three-body models underestimate the experimental cross section is thus explained by their neglect of the backward-propagating pion.

The off-shell extrapolation of the  $\pi N$  scattering amplitudes depends on the underlying  $\pi N$  dynamics one assumes. Lamot *et al.* employed the standard  $\Delta$ -isobar model for  $P_{33}$  scattering. As a result, they obtained a long ranged  $\pi N\Delta$  form factor ( $\Lambda \sim 300$  MeV/ $c$ ), which leads to the strong suppression of the  $N\Delta \rightarrow NN$  transition and hence to the reduction of the  $\pi d \rightarrow NN$  cross section.

We have remedied this unfavorable feature by introducing a nonresonant  $P_{33}$  interaction in addition to the  $\Delta$  resonant interaction. Combined with the effect of the backward-propagating pion, we get the cross section in satisfactory agreement with experiment.

We have also seen that the  $P_{33}$  and  $P_{11}$  half-off-shell functions determined from the  $\pi N$  scattering data are

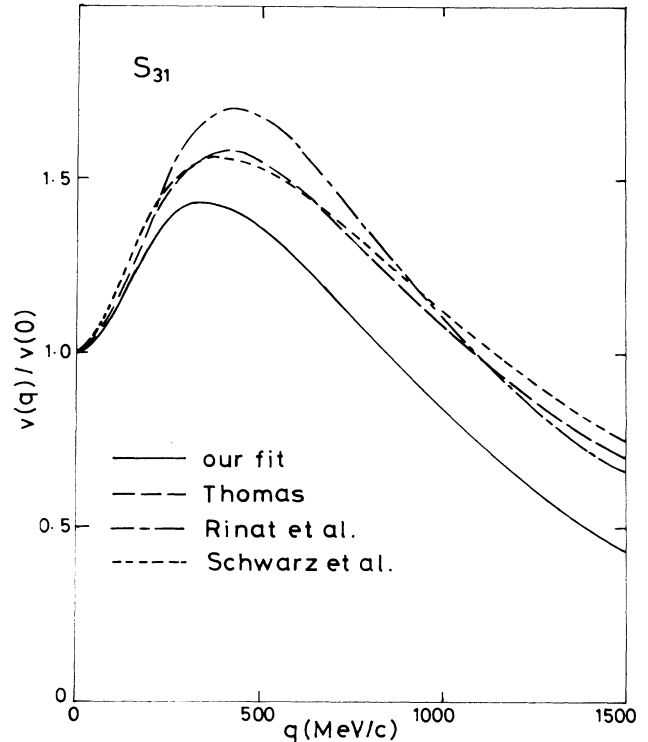


FIG. 9.  $S_{31}$  form factors normalized to one at  $q=0$ . The form factor of Thomas is multiplied by  $\sqrt{2\omega_q}$ .

very similar to the form factor found in the perturbation model ( $\Lambda=600$  MeV/ $c$ ). The above results imply that the perturbation model, in which the cutoff was assumed independently of  $\pi N$  scattering, acquires a justification in the three-body model. In this regards it is important to notice that the higher-order contribution to the total cross section is proved to be small.

To conclude, we have constructed, in the framework of the unitary three-body model, the  $N\Delta$ - $NN$  transition potential from the  $\pi NN$  and  $\pi N\Delta$  vertex interactions deduced from the analyses of the two-body  $\pi N$  scattering data. Based on this model, we have obtained a unified picture for the  $\pi N$  scattering and the  $\pi d \rightarrow NN$  reaction.

#### ACKNOWLEDGMENTS

We would like to thank T. Terasawa for a careful reading of the manuscript. One of us (H.T.) wishes to thank T. Mizutani for helpful discussions. The numerical calculation was performed at the Institute for Nuclear Study, University of Tokyo.

\*Present Address: Institut für Kernphysik, Universität Mainz, D-6500 Mainz, Federal Republic of Germany.

<sup>1</sup>C. Richard-Serre, W. Hirt, D. F. Measday, E. G. Michaelis, M. J. M. Saltmarsh, and P. Skarek, Nucl. Phys. **B20**, 413 (1970).

<sup>2</sup>B. Goplen, W. R. Gibbs, and E. L. Lomon, Phys. Rev. Lett. **32**, 1012 (1974).

<sup>3</sup>W. R. Gibbs, B. F. Gibson, and G. J. Stephenson Jr., in *Meson-Nuclear Physics—1976 (Carnegie-Mellon Conference)*, Proceedings of the International Topical Conference on



- Meson-Nuclear Physics, AIP Conf. Proc. No. 53, edited by P. D. Barnes, R. A. E. Eisenstein, and L. S. Kisslinger (AIP, New York, 1976), p. 464.
- <sup>4</sup>M. Brack, D. O. Riska, and W. Weise, Nucl. Phys. **A287**, 425 (1977).
- <sup>5</sup>J. Chai and D. O. Riska, Nucl. Phys. **A338**, 349 (1980).
- <sup>6</sup>K. Shimizu, A. Faessler, and H. Mütter, Nucl. Phys. **A343**, 468 (1980).
- <sup>7</sup>O. V. Maxwell, W. Weise, and M. Brack, Nucl. Phys. **A348**, 388 (1980).
- <sup>8</sup>J. M. Laget, J. F. Lecomte, and F. Lefebvres, Nucl. Phys. **A370**, 479 (1981).
- <sup>9</sup>M. Hirata, K. Masutani, A. Matsuyama, and K. Yazaki, Phys. Lett. **128B**, 15 (1983).
- <sup>10</sup>W. Grein, A. König, P. Kroll, M. P. Locher, and A. Švarc, Ann. Phys. (N.Y.) **153**, 301 (1984).
- <sup>11</sup>J. Vogelzang, B. L. G. Bakker, and H. J. Boersma, Nucl. Phys. **A452**, 644 (1986).
- <sup>12</sup>A. M. Green and J. A. Niskanen, Nucl. Phys. **A271**, 503 (1976).
- <sup>13</sup>M. Betz and T.-S. H. Lee, Phys. Rev. C **23**, 375 (1981).
- <sup>14</sup>P. U. Sauer, Prog. Part. Nucl. Phys. **16**, 35 (1986).
- <sup>15</sup>E. van Faassen and J. A. Tjon, Phys. Lett. B **186**, 276 (1987).
- <sup>16</sup>B. Blankleider and I. R. Afnan, Phys. Rev. C **24**, 1572 (1981).
- <sup>17</sup>T. Mizutani, C. Fayard, G. H. Lamot, and R. S. Nahabetian, Phys. Lett. **107B**, 177 (1981).
- <sup>18</sup>A. S. Rinat, Y. Starkand, and E. Hammel, Nucl. Phys. **A364**, 486 (1981); A. S. Rinat and Y. Starkand, *ibid.* **A397**, 381 (1983).
- <sup>19</sup>M. Araki, Y. Koike, and T. Ueda, Nucl. Phys. **A389**, 605 (1982).
- <sup>20</sup>I. R. Afnan and R. J. McLeod, Phys. Rev. C **31**, 1821 (1985).
- <sup>21</sup>G. H. Lamot, J. L. Perrot, C. Fayard, and T. Mizutani, Phys. Rev. C **35**, 239 (1987).
- <sup>22</sup>L. D. Faddeev, Zh. Eksp. Teor. Fiz. **39**, 1459 (1960) [Sov. Phys.—JETP **12**, 1014 (1961)].
- <sup>23</sup>I. R. Afnan and A. W. Thomas, Phys. Rev. C **10**, 109 (1974).
- <sup>24</sup>C. Lovelace, Phys. Rev. **135**, B1225 (1964).
- <sup>25</sup>H. Tanabe and K. Ohta, Phys. Rev. Lett. **56**, 2785 (1986); University of Tokyo, Institute for Nuclear Study, Report INS-593, 1986.
- <sup>26</sup>T.-S. H. Lee, Phys. Rev. Lett. **50**, 1571 (1983); Phys. Rev. C **29**, 195 (1984).
- <sup>27</sup>V. Dmitriev, O. Sushkov, and C. Gaarde, Nucl. Phys. **A459**, 305 (1980).
- <sup>28</sup>Y. Avishai and T. Mizutani, Nucl. Phys. **A326**, 352 (1979); **A338**, 337 (1980); **A352**, 399 (1981); Phys. Rev. C **27**, 312 (1983).
- <sup>29</sup>W. N. Cottingham, M. Lacombe, B. Loiseau, J. M. Richard, and R. Vinh Mau, Phys. Rev. D **8**, 800 (1973); M. Lacombe, B. Loiseau, J. M. Richard, R. Vinh Mau, J. Côté, P. Pirès, and R. de Turreil, *ibid.* **21**, 861 (1980).
- <sup>30</sup>J. Haidenbauer and W. Plessas, Phys. Rev. C **30**, 1822 (1984).
- <sup>31</sup>G. E. Brown, A. D. Jackson, and T. T. S. Kuo, Nucl. Phys. **133**, 481 (1969).
- <sup>32</sup>R. A. Arndt, L. D. Roper, R. A. Bryan, R. B. Clark, B. J. VerWest, and P. Signell, Phys. Rev. C **28**, 97 (1983).
- <sup>33</sup>E. Amaldi, S. Fubini, and G. Furlan, in *Pion-Electroproduction*, Vol. 83 of Springer Tracts in Modern Physics (Springer, Berlin, 1979), p. 1.
- <sup>34</sup>R. M. Woloshyn, E. J. Moniz, and R. Aaron, Phys. Rev. C **13**, 286 (1976).
- <sup>35</sup>R. Aaron, D. C. Teplitz, R. D. Amado, and J. E. Young, Phys. Rev. **187**, 2047 (1969).
- <sup>36</sup>T. Mizutani, B. Saghai, C. Fayard, and G. H. Lamot, Phys. Rev. C **35**, 667 (1987).
- <sup>37</sup>R. A. Arndt, J. S. Hyslop III, and L. D. Roper, Phys. Rev. D **35**, 128 (1987).
- <sup>38</sup>D. V. Bugg, J. Phys. G **10**, 47 (1984).
- <sup>39</sup>N. Hiroshige, W. Watari, and M. Yonezawa, Prog. Theor. Phys. **72**, 1146 (1984).
- <sup>40</sup>R. R. Silbar and W. M. Kloet, Nucl. Phys. **A338**, 317 (1980).
- <sup>41</sup>E. van Faassen and J. A. Tjon, Phys. Rev. C **28**, 2354 (1983); **30**, 285 (1984).
- <sup>42</sup>A. B. Laptev and I. I. Strakovsky, Leningrad Nuclear Physics Institute report, 1985.
- <sup>43</sup>D. Aebischer *et al.*, Nucl. Phys. **B106**, 214 (1976).
- <sup>44</sup>J. Hoftiezer *et al.*, Nucl. Phys. **A402**, 429 (1983).
- <sup>45</sup>E. L. Mathie *et al.*, Z. Phys. A **313**, 105 (1983).
- <sup>46</sup>E. Aprile *et al.*, Nucl. Phys. **A379**, 369 (1982); **A415**, 365 (1984).
- <sup>47</sup>A. Saha *et al.*, Phys. Rev. Lett. **51**, 759 (1983).
- <sup>48</sup>T. Mizutani, C. Fayard, G. H. Lamot, and S. Nahabetian, Phys. Rev. C **24**, 2633 (1981).
- <sup>49</sup>A. W. Thomas, Nucl. Phys. **A258**, 417 (1976).
- <sup>50</sup>K. Schwarz, H. F. K. Zingl, and L. Mathelitsch, Phys. Lett. **83B**, 297 (1979).